The tissue diagnostic instrument

Paul Hansma,[1] Hongmei Yu,[2] David Schultz,[3] Azucena Rodriguez,[3] Eugene A. Yurtsev,[1] Jessica Orr,[3] Simon Tang,[3] Jon Miller,[4] Joseph Wallace,[5] Frank Zok,[6] Cheng Li,[7] Richard Souza,[8] Alexander Proctor,[9] Davis Brimer,[9] Xavier Nogues-Solan,[10] Leonardo Mellbovsky,[10] M. Jesus Peña,[10] Oriol Diez-Ferrer,[10] Phillip Mathews,[1] Connor Randall,[1] Alfred Kuo,[3] Carol Chen,[3] Mathilde Peters,[4] David Kohn,[5] Jenni Buckley,[3] Xiaojuan Li,[8] Lisa Pruitt,[7] Adolfo Diez-Perez,[10] Tamara Alliston,[3] Valerie Weaver,[2] and Jeffrey Lotz[3]

[1]*Department of Physics, University of California, Santa Barbara, California 93106, USA*
[2]*Department of Surgery, Department of Anatomy, Department of Bioengineering and Therapeutics, and Center for Bioengineering and Tissue Regeneration, University of California, San Francisco, California 94143, USA*
[3]*Department of Orthopaedic Surgery, University of California, San Francisco, California 94143, USA*
[4]*Department of Dentistry, University of Michigan, Ann Arbor, Michigan 48109, USA*
[5]*Department of Biologic and Materials Sciences and Department of Biomedical Engineering, University of Michigan, Ann Arbor, Michigan 48109, USA*
[6]*Department of Materials, University of California, Santa Barbara, California 93106, USA*
[7]*UC Berkeley and UCSF Joint Graduate Group in Bioengineering, Berkeley, California 94720, USA*
[8]*Department of Radiology and Biomedical Imaging, University of California, San Francisco, California 94143, USA*
[9]*Active Life Technologies, 629 State St., Suite 213, Santa Barbara, California 93101, USA*
[10]*Hospital del Mar, Department of Internal Medicine, Autonomous University of Barcelona, P. Maritim 25-29, 08003 Barcelona, Spain*

(Received 11 December 2008; accepted 13 April 2009; published online 27 May 2009)

Tissue mechanical properties reflect extracellular matrix composition and organization, and as such, their changes can be a signature of disease. Examples of such diseases include intervertebral disk degeneration, cancer, atherosclerosis, osteoarthritis, osteoporosis, and tooth decay. Here we introduce the tissue diagnostic instrument (TDI), a device designed to probe the mechanical properties of normal and diseased soft and hard tissues not only in the laboratory but also in patients. The TDI can distinguish between the nucleus and the annulus of spinal disks, between young and degenerated cartilage, and between normal and cancerous mammary glands. It can quantify the elastic modulus and hardness of the wet dentin left in a cavity after excavation. It can perform an indentation test of bone tissue, quantifying the indentation depth increase and other mechanical parameters. With local anesthesia and disposable, sterile, probe assemblies, there has been neither pain nor complications in tests on patients. We anticipate that this unique device will facilitate research on many tissue systems in living organisms, including plants, leading to new insights into disease mechanisms and methods for their early detection. © *2009 American Institute of Physics.*
[DOI: 10.1063/1.3127602]

I. INTRODUCTION

The tissue diagnostic instrument (TDI) was redesigned from the bone diagnostic instrument[1,2] so as to measure tissue mechanical properties subcutaneously and *in vivo* with additional probe assemblies and an adjustable compliance (Fig. 1). It consists of a thin probe assembly that can penetrate skin and soft tissue to reach deep tissues. The disposable, sterilizable probe assembly consists of an outer reference probe made from a 23 gauge hypodermic needle and an inner test probe made from stainless steel wire ranging from 175 to 300 μm in diameter and from 2 to 90 mm in length. Since friction between the test probe and the reference probe increases with length, it is desirable to use only the length needed to access the desired tissue location. The test probe is held in a nickel tube that couples to a magnet, which in turn is linked to a force generator. During operation the force generator oscillates the probe within the tissue of interest and concurrently measures the force and displacement. The maximum values for force and displacement are 12 N and 600 μm. The probe is typically operated at a frequency of 4 Hz because this is rapid enough to allow hand holding yet sufficiently slow to allow easy decoupling of the elastic and viscous response of the tissue (see supplementary material[3] for more details including force and displacement ranges.)

II. MEASUREMENTS

We first illustrate TDI use in human spinal disks that are composed of a thick outer ligament (*annulus fibrosus*) and a central swelling hydrogel (*nucleus pulposus*). Spinal disk degeneration can be the underlying cause of back pain leading to significant morbidity and societal expense. Intervertebral disks are one of the most highly loaded tissues in the body, and consequently material property insufficiency can lead to damage accumulation, inflammation, and pain. Disk degen-

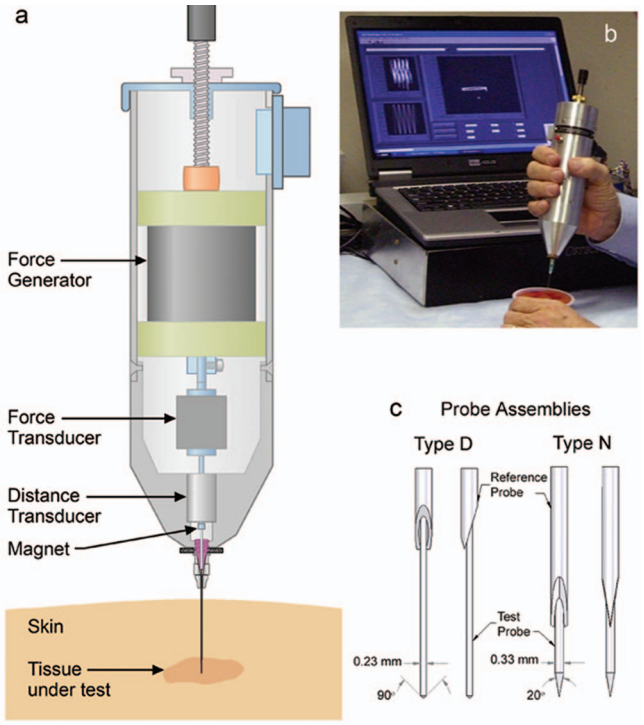

FIG. 1. (Color) The TDI. (a) The TDI can measure mechanical properties of tissues under test even if they are covered with skin and other soft tissues because it has a probe assembly that can be inserted subcutaneously into the tissue under test. (b) It can be handheld and is connected to a computer for data generation, acquisition, and processing. In this photo it is being used to measure differences in the mechanical properties of fruit and gel in a snack food. (c) A probe assembly for the TDI consists of a test probe, which moves displacements of the order of 200 μm relative to the reference probe. The reference probe serves to shield the test probe from the influence of the skin and soft tissue that must be penetrated to reach the tissue under test. Type D probes are good for very soft tissue, such as the murine breast tissue in Fig. 3. Type N probes are good for stiffer tissue, such as the spinal disk tissue in Fig. 2. The screw at the top of the TDI (a) can adjust the compliance of the TDI, as discussed in the supplementary material.

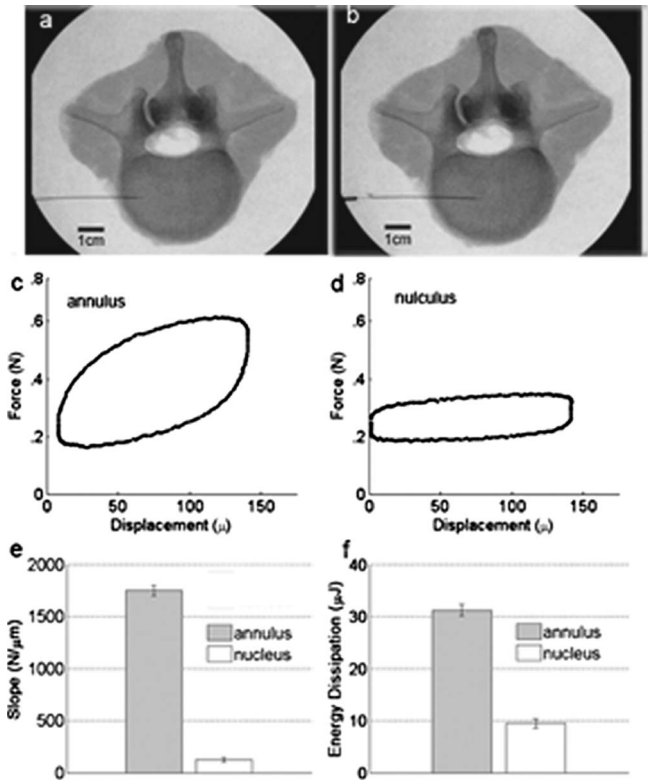

FIG. 2. Demonstration of the ability of the TDI to distinguish between the annulus and nucleus of a human intervertebral disk. (a) X-ray image of transverse view of a cadaver lumbar motion segment L12 with test probe located in annulus. (b) Similar view with probe centered in the nucleus. (c) Force vs displacement curve measured by the TDI during a cyclic load cycle (4 Hz) in the annulus. (d) Force vs displacement curve measured in the nucleus. Note that the annulus is much stiffer (higher slope) and dissipates more energy (higher area enclosed by the curve). (e) Histogram comparing the average least-squares slope for ten cycles in the annulus vs in the nucleus. (f) Histogram comparing the average energy dissipation for ten measurements in the annulus vs in the nucleus (31.8 ± 1.1 μJ vs 9.7 ± 0.6 μJ; $p < 0.01$). The error bars indicate standard deviation for the ten measurements within the annulus and within the nucleus in the disk.

eration is currently diagnosed using imaging techniques, such as magnetic resonance.[4] Unfortunately, these methods can only indirectly suggest disk mechanical properties, which currently cannot be measured *in vivo*.

Using image-guided, percutaneous placement [Figs. 2(a) and 2(b)], disk material properties can now be measured safely *in vivo* using a type N probe assembly [Fig. 1(c)]. The novel sharpening of the reference probe for type N probe assembly decreases the problem of tissue being caught between the test probe and the reference probe during insertion and thus decreases the friction between the test probe and the reference probe. The friction between the test and reference probes is typically ~0.02 N. The specific value is recorded by the software before testing a sample and is removed from the samples' force versus distance plot before analysis. The force versus displacement data are plotted in real time and recorded digitally [Figs. 2(c) and 2(d)]. The slope of the force versus displacement curve provides a measure of disk elasticity: in the case of a simple spring, the slope would be the spring constant. The energy dissipation in the force versus displacement curve is the area inside the curve and is a measure of the viscous behavior. Viscosity is absent from a simple spring yet is large for a purely viscous material such as petroleum jelly, which has an elasticity near zero.

There are significant differences (p values of <0.01) in slope (N/m) and energy dissipation (μJ) between the *annulus fibrosus* and the *nucleus pulposus* (Fig. 2). The *annulus fibrosus* has both higher slope and energy dissipation. These results are representative of our measurements on 11 disks: the slope and energy dissipation are always greater in the annulus than the nucleus. This observation of higher slope or stiffness in the annulus is consistent with previous experiments measuring the compressive properties of both annulus and nucleus.[5,6] However, a precise comparison with established mechanical data is not readily available because mechanical testing in this manner at high spatial resolution has not been possible previously. Because these properties are known to change with age and degeneration, an eventual goal would be to determine whether *in vivo* measures of annulus and nucleus material properties provide novel data that improve back pain diagnosis and treatment. We note that the 23 gauge needle is consistent with the recent recommendation[7] that a spinal needle smaller than or equal to 22 gauge should be used to prevent postsurgery leakage.

An epithelial tissue such as the mammary gland is an

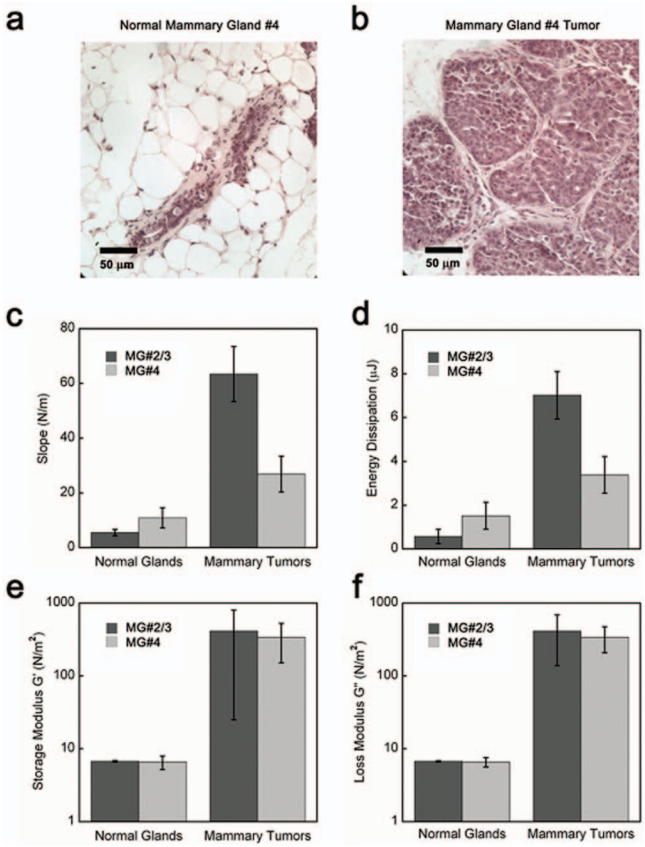

FIG. 3. (Color) Demonstration of the ability of the TDI to distinguish between normal mammary glands and tumors. Hematoxylin and eosin (H&E) staining of (a) the representative normal FVB murine mammary gland and (b) the matched malignant MMTV-PyMT+/-murine mammary gland that were tested in this experiment. (c) The mammary tumors have significantly ($P<0.001$) higher slopes, a measure of elasticity, for both the thoracic # 2/3 and the inguinal #4 tissues. (d) The mammary tumors have significantly higher energy dissipation for the thoracic # 2/3 tissue ($P<0.001$), but the difference for the inguinal # 4 tumor was not significant. Histogram comparing (e) the elastic modulus and (f) the loss modulus, as measured by rheology, for the normal mammary glands and mammary tumors after the TDI measurements (two subregions for each mammary gland, ten measurements for each region). Note that the results for elasticity and loss modulus for the two techniques reproduce the same general trends. The error bars in the measurements indicate standard deviation for all the measurements.

example of the softest tissue that can be probed with the current TDI. Figure 3 shows a paired-comparison of the mammary glands #2/3 and #4 from normal Friend Virus B, mice and tumors arising in the matched mammary glands of their MMTV-PyMT+/- (Mouse Mammery Tumor Virus-Polyoma Middle T Antigen) littermates. These data are representative of the data in an ongoing study of various tumors. The results of that study are beyond the scope of this paper, but we can report that all 30 tumors are stiffer (have higher slope) than all 15 normal mammary glands in tissue site-matched and age-matched mice. Normal murine mammary glands have elastic modulus below 1 kPa as measured with a conventional rheometer and with the TDI device. This value is comparable with our calibration curves on polyacrylamide (PA) gels (see supplementary material) that demonstrate TDI sensitivity below 1 kPa. Normal and transformed human breast tissue is considerably stiffer than mouse tissue[8] and is therefore well within the range of the TDI. Tissue stiffness increases in many breast cancers. To quantify stiffness and improve breast tumor detection, imaging modalities such as sonoelastography and Magnetic Resonance elastography have been used.[9,10] The TDI offers a tractable and economical approach to measure breast stiffness *in situ* with millimeter resolution. Our preliminary trials on human breast tissue from cadavers showed detectable variations in mechanical properties between different locations in the same specimen with a spatial resolution of 2 mm (data not shown). Based on these observations an eventual goal would be to use the TDI for localization of human breast cancer *in situ*. A foreseeable clinical application includes using the device to define margins of affected tissue and sites for biopsy. The TDI measurement could easily be combined with biopsy; the test probe could be withdrawn into the reference probe to collect a biopsy sample after mechanical testing. We are currently investigating the molecular mechanism of how the mechanical properties contribute to breast cancer; the TDI can be applied to clarify the molecular link between matrix materials properties of tissues and tumor risk (i.e., breast cancer in women with mammographically dense breasts[11,12]).

Prior to clinically apparent symptoms of osteoarthritis, the material quality and mechanical function of cartilage matrix are compromised.[13] The ability to noninvasively probe the material quality of this stratified tissue will complement and extend current diagnostic capabilities.[13] Furthermore, detection of cartilage degeneration early in osteoarthritis may increase the success of therapeutic intervention. To that end, the ability of the TDI to distinguish the elastic modulus of synthetic materials with moduli comparable to cartilage was validated against well-established methods including atomic force microscopy, nanoindentation, and bulk stress relaxation (Fig. 4). In addition to accurately measuring the elastic modulus of PA gels with a range of moduli from 0.2 to 1 MPa, the TDI could measure the elastic modulus of a stiff gel that was inferior to a compliant gel, demonstrating its ability to noninvasively evaluate a stratified material [Fig. 4(d)]. When applied to cartilage, the TDI readily discriminated between a young healthy cadaveric specimen and an old degenerated surgical specimen that were probed *in situ* [Fig. 4(f)].

Human dentin is an example of the hard tissue that can be probed with our current device (Fig. 5). One unsolved problem for practicing dentists is deciding when a sufficient depth has been reached when drilling to remove carious dentin from a cavity. One proposed solution has been the development of a new experimental polymer bur (from SS White Burs, Inc., Lakewood, NJ), which is designed to remove soft decaying dentin but blunt on harder healthy dentin and thus self-limit the tissue amount removed. Here we show the properties of the remaining dentin after a first excavation by such a bur and then after a second excavation with a second polymer bur of the same type (Fig. 5). Next was a third excavation with a #4 round carbide bur and finally a cavity preparation into presumably sound dentin using a #330 carbide bur. Note that even after the cavity preparation, the dentin did not have the full elastic modulus of the healthy dentin. Our primary focus was on relative values as excavation proceeded. The elastic modulus, as calculated from force

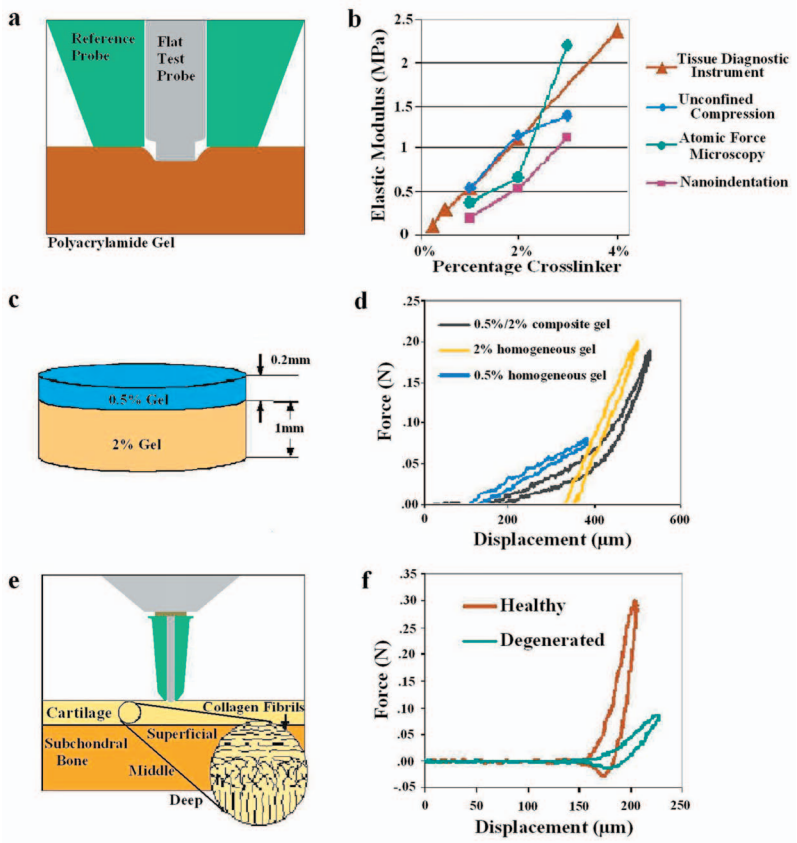

FIG. 4. (Color) Demonstration of the ability of the TDI to distinguish differences in moduli of stratified materials such as cartilage. (a) The elastic modulus can be determined with the type V probe assembly that indents soft materials rather than penetrating them, as above. (b) PA gels with elastic moduli in the range previously reported for cartilage (0.2–1 MPa) were used to validate the TDI relative to other established methods, including atomic force microscopy, nanoindentation, and bulk stress relaxation. PA gel moduli increased dose-dependently with cross-linker concentration ($p=0.012$). (c) To construct a stratified elastic modulus gel, a 0.2 mm thick layer of "compliant" PA gel was poured over a prepolymerized 1 mm thick "stiff" PA gel. (d) The force vs displacement curve produced by the TDI revealed two distinct slopes on the loading curve for the stratified gels. Each slope of the composite gel matches the corresponding slopes for homogeneous 0.5% and 2% PA gel, demonstrating the capability to analyze stratified materials, such as cartilage. (e) A schematic of the indentation tests performed on cartilage, which were performed in hydrated conditions with phosphate buffered saline. (f) Using similar test conditions, the TDI easily distinguished between young cadaveric cartilage and aged degenerated cartilage measured *in situ*.

versus displacement curves generated by the TDI and analyzed using a modified Oliver and Pharr[14] method, for the dentin left in the cavity by the polymer bur was below that for healthy dentin far from the cavity [Fig. 5(c)]. Please see the appendix for the details of the modified method. The hardness, as calculated from force versus displacement curves generated by the TDI and analyzed using a modified Oliver and Pharr[14] method, for the dentin left in the cavity by the polymer bur was below that for healthy dentin far from the cavity [Fig. 5(c)]. One-way analysis of variance gives values of $P<0.0001$ for the elastic modulus and $P=0.0008$ for the hardness, indicating that the variation among means is significantly greater than expected by chance. Thus the TDI has the potential to quantify the properties of dentin left in a cavity and could be used to study the outcome of various treatment strategies for how much degenerated dentin is removed before filling the cavity.

The absolute value for the elastic modulus of our "healthy dentin" is well within the range of existing measurements but below the value of 20–25 GPa recommended in a recent critical reevaluation of the literature.[15] The reason is probably the storage of the teeth in water for weeks before measurement.[16] To our knowledge, the TDI is the first instrument that can measure elastic modulus and hardness inside irregularly shaped, fully hydrated dentin cavities. It could be used for research projects without further modification. For individual clinical use, a smaller, less expensive version with an angled probe would be desirable. The experiments on dentin reported here build on a rich history of measuring mechanical properties with indentation methods.[14,17,18] Of special interest is recent work modeling size effects with finite element analysis[19] because extensions of work such as this may lead to a more quantitative understanding of TDI measurements on soft tissue as well as hard tissue.

The hard tissue, bone, is of particular interest medically because of the growing incidence of debilitating bone fracture as our population ages.[20] Changes in bone material properties are believed to play a role in fracture risk.[21–23] With the top screw backed off, as discussed in the supplementary materials,[3] the TDI functions as a Bone Diagnostic Instrument,[1,2] which may, after clinical tests, prove useful in quantifying the component of bone fragility due to degraded material properties. Figure 6 shows tests of the TDI, working as a bone diagnostic instrument, on a living patient to determine if the procedure is painful or results in complications. Neither this patient nor the others tested to date experienced

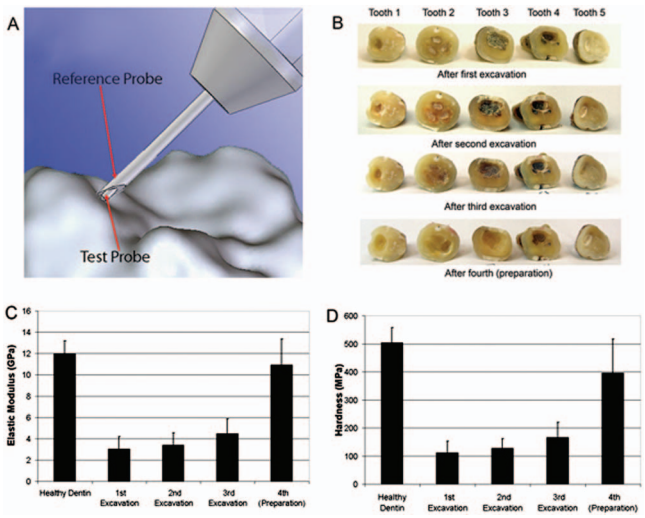

FIG. 5. (Color) Demonstration of the ability of the TDI to measure the elastic modulus and hardness of human dentin to quantify the properties of the dentin left in a tooth cavity after each of multiple excavations and finally preparation. (a) The probe assembly for these measurements was designed to indent the hard tissue. The reference probe was a hypodermic needle that rested on the surface under test. The test probe was sharpened into a 90° cone with a 30 μm radius at the end (drawing by Haykaz Mkrtchyan). (b) The teeth after the various excavations and finally preparation. At each successive stage of excavation and preparation more dentin was removed from the cavity. [(c) and (d)] The elastic modulus and hardness of the dentin remaining in the cavity was significantly ($p=.01$) less than that of healthy dentin. The error bars indicate standard deviation of the ten measurements that were taken on each of the five teeth (a total of 50 measurements). Note that the elastic modulus of the healthy dentin is over 10 GPa, over seven orders of magnitude greater than the normal mammary glands (Fig. 3), demonstrating the range of the TDI.

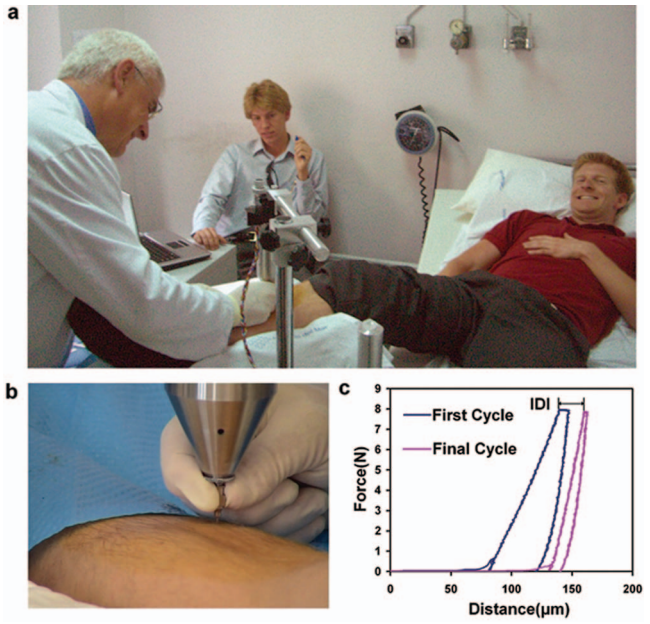

FIG. 6. (Color) Demonstration of the ability of the TDI to do measurements on a living patient. (a) The probe assembly of the TDI is lowered by a physician (A.D.P.) to penetrate the skin and soft tissue covering the tibia of the patient (D.B.) after the test site has been sterilized and locally anesthetized. (b) Close up of the physician's hand on the probe assembly as he lowers it to the bone surface. (c) Representative force vs distance curves measured on the bone of the patient. This patient and the other patients tested to date experienced neither pain nor complications with the procedure. The most important parameter is the indentation distance increase (IDI) defined in the image as the increase in indentation distance from the first cycle to the last. In model systems the IDI is greater for more easily fractured bone. Other parameters such as the creep at nearly constant force (the plateau on the top of the curves), the elastic modulus, the energy dissipation, and the hardness can also be determined from analysis of the force vs distance curves.

any pain beyond the initial "stick" when the local anesthesia was injected. There have been no complications.

III. DISCUSSION OF NEW POSSIBILITIES

It might, in the future, be possible for the TDI to measure the interaction forces between antibody coated test probes and tissues. This would allow measurements of single molecule interactions as is currently achieved with an atomic force microscope.[24] Rupture forces in the range of 20–140 pN have been measured for many receptor-ligand interactions with single-cell force spectroscopy.[25] With these interaction forces, we can make order of magnitude estimates of forces we might find when trying to rotate or translate a test probe that had bound to a tissue with many molecular bonds in parallel. Assuming a molecular density of 1 molecule/10 nm^2, an interaction force per molecule of 50 pN, a coated region of area of 4×10^{-6} m^2 (the exposed area of the type D probe), and a fractional binding of 1%, we would get a force of 50 pN/molecule $\times 4\times10^{-6}$ m^2 $\times 1$ molecule/10 $nm^2\times.01=200$ mN. The present lower limits of sensitivity of the TDI for forces come from the friction between the test probe and the reference probe, of the order of 10 mN, and from the force noise in our force transducer, of the order of 5 mN in a 1 kHz bandwidth. Thus forces of the magnitude that could be expected from molecular interactions with coated tips should be measurable. A big problem could be nonspecific interaction masking specific interactions. A proof of concept experimental approach to overcoming this masking effect would be to use a test probe coated on just one side that was exposed to the tissue under test through a window in the wall of a closed-end reference probe. The difference in the forces between the test probe and the tissue under test for the coated versus uncoated side could be measured. This could naturally be extended with multiple coatings on multiple strips on the test probe, each exposed one by one through a slit in the wall of the closed-end reference probe. We emphasize, however, that proof of concept experiments will be necessary to evaluate this potential application of the TDI.

It is important to note that though the present instrument is able to make basic measurements in a wide range of tissues (almost all tissues in the human body from very soft breast tissue to hard, mineralized tissues), it is in a very early stage of development. More versatile instruments with more measurement modalities, such as mentioned above, and more user convenience features, such as wireless operation, are possible. Specialized instruments for specific measurements in specific tissues could be developed at a small fraction of the cost of the fully versatile instrument. The device could also be modified to assess materials properties of various bioengineered artificial three dimensional tissues.[26,27]

ACKNOWLEDGMENTS

We thank the NIH for support of this work under Grant Nos. RO1 GM 065354 and RO1 AR 049770 and NIH Grant

No. AR049770, the DOD under Grant No. W81XWH-05-1-330, and the Fondo de Investigaciones Sanitarias (FIS) under Grant No. PI07/90912. We thank Angus Scrimgeour for asking us to do indentation measurements on bone, Robert Recker for encouraging us to plan for clinical trials even when the BDI was at an early stage of development, Paul Zaslansky for pointing us toward dental applications, and Georg Fantner, Jonathan Adams, Patricia Turner, Doug Rhen, Jason Lelujian, and Ralf Jungman for helping develop prototype BDIs, which then stimulated development of the more general TDI.

[1] P. K. Hansma, P. J. Turner, and G. E. Fantner, Rev. Sci. Instrum. **77**, 075105 (2006).
[2] P. Hansma, P. Turner, B. Drake, E. Yurtsev, A. Proctor, P. Mathews, J. Lelujian, C. Randall, J. Adams, R. Jungmann, F. Garza-de-Leon, G. Fantner, H. Mkrtchyan, M. Pontin, A. Weaver, M. B. Brown, N. Sahar, R. Rossello, and D. Kohn, Rev. Sci. Instrum. **79**, 064303 (2008).
[3] See EPAPS Document No. E-RSINAK-80-032905 for details regarding the measurements and test methods of the TDI on various biomaterials. For more information on EPAPS, see http://www.aip.org/pubservs/epaps.html.
[4] C. W. A. Pfirrmann, A. Metzdorf, M. Zanetti, J. Hodler, and N. Boos, Spine **26**, 1873 (2001).
[5] S. M. Klisch and J. C. Lotz, J. Biomech. **32**, 1027 (1999).
[6] J. M. Cloyd, N. R.Malhotra, L. Weng, W. Chen, R. L. Mauck, and D. M. Elliott, Eur. Spine J. **16**, 1892 (2007).
[7] J. L. Wang, Y. C. Tsai, and Y. H. Wang, Spine **32**, 1809 (2007).
[8] G. D. A. Sarvazyan, E. Maevsky, and G. Oranskaja, Proceedings of the International Workshop on Interaction of Ultrasound with Biological Media, 1994, Valenciennes, France, p. 6981.
[9] A. Samani, J. Zubovits, and D. Plewes, Phys. Med. Biol. **52**, 1565 (2007).
[10] A. Samani and D. Plewes, Phys. Med. Biol. **52**, 1247 (2007).
[11] M. J. Paszek, N. Zahir, K. R. Johnson, J. N. Lakins, G. I. Rozenberg, A. Gefen, C. A. Reinhart-King, S. S. Margulies, M. Dembo, D. Boettiger, D. A. Hammer, and V. M. Weaver, Cancer Cells **8**, 241 (2005).
[12] N. F. Boyd, H. Guo, L. J. Martin, L. M. Sun, J. Stone, E. Fishell, R. A. Jong, G. Hislop, A. Chiarelli, S. Minkin, and M. J. Yaffe, N. Engl. J. Med. **356**, 227 (2007).
[13] R. U. Kleemann, D. Krocker, A. Cedraro, J. Tuischer, and G. N. Duda, Osteoarthritis Cartilage **13**, 958 (2005).
[14] W. C. Oliver and G. M. Pharr, J. Mater. Res. **19**, 3 (2004).
[15] J. H. Kinney, S. J. Marshall, and G. W. Marshall, Crit. Rev. Oral Biol. Med. **14**, 13 (2003).
[16] S. Habelitz, G. W. Marshall, M. Balooch, and S. J. Marshall, J. Biomech. **35**, 995 (2002).
[17] W. D. Nix and H. J. Gao, J. Mech. Phys. Solids **46**, 411 (1998).
[18] W. C. Oliver and G. M. Pharr, J. Mater. Res. **7**, 1564 (1992).
[19] Y. Huang, F. Zhang, K. C. Hwang, W. D. Nix, G. M. Pharr, and G. Feng, J. Mech. Phys. Solids **54**, 1668 (2006).
[20] Z. A. Cole, E. M. Dennison, and C. Cooper, Osteoporosis Epidemiology Update, Curr. Rheumatol. Rep. **10**, 92 (2008).
[21] E. Durchschlag, E. P. Paschalis, R. Zoehrer, P. Roschger, P. Fratzl, R. Recker, R. Phipps, and K. Klaushofer, J. Bone Miner. Res. **21**, 1581 (2006).
[22] H. S. Gupta, P. Fratzl, M. Kerschnitzki, G. Benecke, W. Wagermaier, and H. O. K. Kirchner, J. R. Soc., Interface **4**, 277 (2007).
[23] R. K. Nalla, J. J. Kruzic, J. H. Kinney, and R. O. Ritchie, Bone **35**, 1240 (2004).
[24] M. Rief, F. Oesterhelt, B. Heymann, and H. E. Gaub, Science **275**, 1295 (1997).
[25] J. Helenius, C. P. Heisenberg, H. E. Gaub, and D. J. Muller, J. Cell Sci. **121**, 1785 (2008).
[26] L. G. Griffith and M. A. Swartz, Nat. Rev. Mol. Cell Biol. **7**, 211 (2006).
[27] J. G. Jacot, S. Dianis, J. Schnall, and J. Y. Wong, J. Biomed. Mater. Res. Part A **79A**, 485 (2006).